Non-contact Thermometry

DOI: 10.1002/anie.201302449

Wide-Range Temperature Sensing using Highly Sensitive Green-Luminescent ZnO and PMMA-ZnO Film as a Non-Contact Optical Probe**

*Satish Laxman Shinde and Karuna Kar Nanda**

In the era of micro/nanotechnology, measurement of temperature with micro/nanometer-scale spatial resolution is very crucial. Various nanothermometers have been developed, such as liquid-in-tube nanothermometers based on the thermal expansion of a liquid in nanotubes,[1] nanoscale thermocouples,[2,3] fluorescence thermometers based on temperature-dependent luminescence of nanostructures,[4–6] IR thermometers based on metal nanostructures,[7] and nanothermometers based on the increase in size of the nanostructures.[8] Among these nanothermometers, the fluorescence-based version is gaining popularity because of the wide range of applications. The temperature can be monitored by probing the luminescence properties, such as absolute and relative emission intensities, excited state lifetime, and peak positions.[9,10] The materials investigated for luminescent thermometry are nano/micro particles, quantum dots, organic dyes, phosphors/polymers, and so on.[9,10] These thermometers have an accuracy of 0.1 K and sensitivity of 0.03–19.6 % K^{-1},[10] which give them wide range of applications, such as scanning thermal microscopy, microfluidic, biological imaging, monitoring the temperature of fast moving turbine blades and aircrafts, temperature-induced phase transition studies, temperature mapping of surfaces, thermal therapies, and intracellular temperature mapping.[11–20]

Recently, it has been demonstrated that the temperature-dependent band gap of ZnO (through transmittance studies) can be explored to evaluate the temperature in a wide range (300–773 K).[21] Such thermometers have restricted applications, as the transmittance/absorbance spectra used for the evaluation of the band gap are recorded in dark. Furthermore, precise measurement of the band gap is difficult and the resolution is 1 K. Herein, we present the synthesis of ZnO microcrystals with a very weak (almost quenched) ultraviolet (UV) emission but a strong green emission by vaporizing Zn and quenching the product. We show that the individual or ZnO microcrystallite powder can be used for sensing and mapping of temperature in a wide range (83–473 K) with an accuracy of 0.1 K and sensitivity better than that previously reported. We have shown that ZnO embedded in poly(methyl methacrylate) (PMMA), which is a transparent thermoplastic polymer often used as a glass substitute, can also be used in thermometry. We have evaluated the temperature profile of a carbon nanotube (CNT) mat generated by Joule heating and shown the possibility of the temperature mapping. Overall, our results clearly demonstrate another application space of ZnO in cryogenic thermometry using green-luminescent micro/nanoparticles and can be used for a wide range of applications.

Green-luminescent ZnO microcrystals were obtained by vaporizing Zn powder at high temperature and quenching the product (Supporting Information, Figures S1–S3). The normalized PL spectra taken at room temperature (293 K) of ZnO microcrystallites (ZnO), individual microcrystals (ZnO′), and ZnO in PMMA (PMMA-ZnO) are shown in Figure 1 a. A strong defect-related green and a very weak (almost negligible) UV band are observed. The UV and green band are centered around 394 and 515 nm, respectively. It is interesting to note that the peak positions remain unchanged even for ZnO in PMMA. The slight improvement of UV to

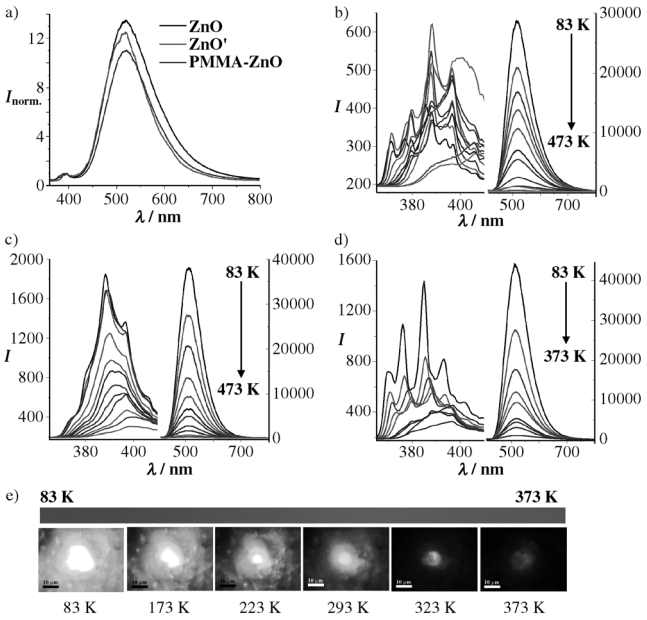

Figure 1. a) Normalized photoluminiscence (PL) spectra and b)–d) temperature-dependent PL of ZnO, ZnO′, and PMMA-ZnO. Spectra were acquired in 40 K steps. e) Optical images of PMMA-ZnO at different temperatures (83–373 K) when exposed to 355 nm. Scale bars: 10 μm.

[*] S. L. Shinde, Prof. K. K. Nanda
Materials Research Centre, Indian Institute of Science
Bangalore-12 (India)
E-mail: nanda@mrc.iisc.ernet.in

[**] The authors acknowledge the financial support from Department of Science and Technology (DST) through Nanomission. The authors also acknowledge Dr. Enda McGlynn and Dr. Balaram Sahoo for their valuable comments and suggestions. PMMA = poly(methyl methacrylate).

Supporting information for this article is available on the WWW under http://dx.doi.org/10.1002/anie.201302449.

visible luminescence is due to surface modification. Generally, ZnO exhibits various defects such as oxygen vacancy (V_o), Zn vacancy (V_{Zn}), oxygen interstitial (O_i), and Zn interstitial (Zn_i). V_o and V_{Zn} are the most dominant defects in ZnO, which introduces various trap levels in the forbidden region between the valence band and conduction band.[22–25] Although the UV emission is due to the recombination of free excitons, the green emission is attributed to transitions at a V_O defect.[22,23] Quenched ZnO have excess oxygen vacancies resulting in strong green emission.

The temperature-dependent PL spectra recorded in a broad range of cryogenic temperature (83–473 K) for ZnO, ZnO′, and PMMA-ZnO are shown in Figure 1 b–d. Overall, the UV band shifts from 3.21 to 3.07 eV, while the green band shifts from 2.40 to 2.38 eV as the temperature is raised from 83 to 473 K, which is in accordance with reported results.[26,27] Apart from the blue shift at low temperatures, fine structures are also observed in the UV region. The peaks observed at 371, 377, 380, 386, 388, 394, and 397 nm are due to free excitons and their longitudinal optical (LO) phonon replicas.[26–31] It may be noted that the resolution of the fine structures of UV band for ZnO′ is very weak as compared to ZnO and PMMA-ZnO (Figure 1 b–d). The possible explanations are discussed in the Supporting Information, Figure S4. Optical images of luminescence of PMMA-ZnO at different temperatures (83–373 K) are shown Figure 1 e. It is apparent that the intensity of green band decreases with increasing temperature.

Figure 2 a–c shows the dependency of PL peak intensities with temperature for ZnO, ZnO′, and PMMA-ZnO, respectively. It may be noted that the variation of green band intensity is stronger compared to that of the UV band. The ratio of the green to UV band intensity is shown in the insets of Figure 2 a–c, which clearly reveal a monotonic increase as the temperature is decreased. For ZnO (obtained by slow cooling) with strong UV luminescence, the variation of UV intensity with temperature is stronger compared to the green band (Supporting Information, Figure S5 a–c). Overall, the PL and the variation in the intensities can be controlled by varying the synthesis parameters, such as growth temperature or cooling rate, through defects.

This different variation of UV and green band intensity with temperature suggests the possibility of ratiometric temperature sensing. Non-contact optical temperature measurement may be realized by taking the intensity ratio R of UV (I_{UV}) and the green band (I_G). The absolute sensitivity (S) and the relative sensitivity (S_R) of ratiometric thermometer is defined as:[9,10]

$$S = dR/dT \text{ and } S_R = S/R \quad (1)$$

The variation of S and S_R with temperature for ZnO, ZnO′, and PMMA-ZnO are shown in Figure 2 d. The variation of absolute sensitivity (S*) and the relative sensitivity (S_R*) evaluated by the previously described procedure[6,9] is shown in the Supporting Information, Figure S6. The S and S* values in the temperature range of 83–473 K are listed in the Supporting Information, Table S1 and the maximum S and S_R of ZnO with reported results is compared in Table S2. Because of the high stability and moderate sensitivity, the application of PMMA-ZnO in cryogenic thermometry is highly recommended.

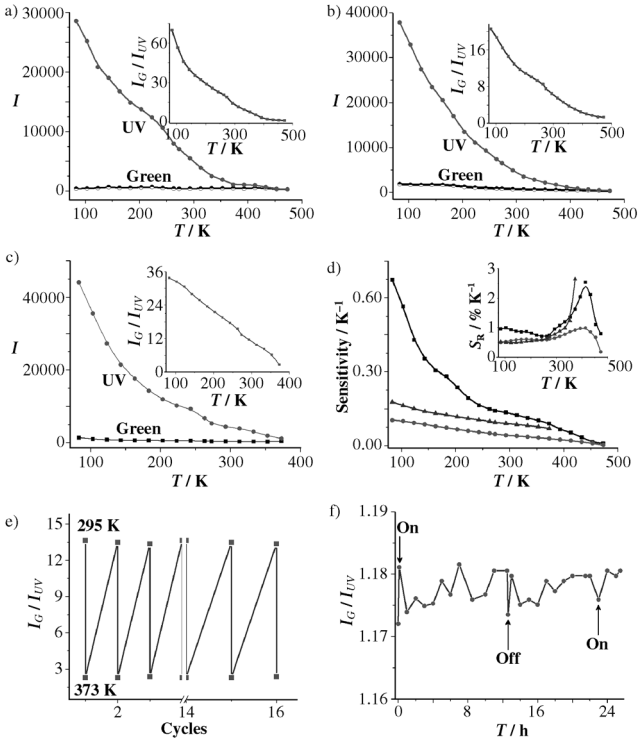

Figure 2. a)–c) Temperature-dependent peak intensity of green and UV band and the ratio (inset) of ZnO, ZnO', and PMMA-ZnO, and d) the absolute sensitivity and the relative sensitivity (inset) as a function of temperature. ■ ZnO, ● ZnO', ▲ PMMA-ZnO. e) Variation of intensity ratio of ZnO at 295 and 373 K measured over a span of four months. The variation is within 1 %. f) Variation of intensity ratio of ZnO with time at 448 K without (off) and with (on) vacuum.

It may be noted that the I_G/I_{UV} intensity ratio for ZnO is decreased from 67 to 1 as temperature varied from 83 to 473 K, which indicates a temperature resolution of about 0.1 K. As the excitation wavelength is 355 nm and the numerical aperture of objective lens of microscope is 0.6, the spatial resolution is about 600 nm, which is consistent with the experimental results.[10,32] A comparison of the spatial resolution with that of different thermometers reported in the literature is provided in the Supporting Information, Table S3. To evaluate the thermal stability of ZnO, we have performed two set of experiments. Recycle test has been performed at 298 and 373 K in a span of four months and the results are shown in Figure 2 e. To study the thermal stability at higher temperature with different oxygen partial pressure, the intensity ratio with time is recorded. Temporal response curve for ZnO at 448 K without and with vacuum (ca. 10^{-4} mbar) is shown in Figure 2 f, which shows a very slight (almost negligible) variation in intensity ratio with different oxygen partial pressure at least for 26 h. The results shown in Figure 2 clearly indicate that the materials qualify for temperature sensing.

It has been well-established that the temperature of a CNT mat increases when voltage is applied across it.[33] To

evaluate the temperature profile and perform temperature mapping throughout the mat, it is placed on a SiO_2 wafer with Ag electrodes on top. The ZnO microcrystals are then drop-casted over the mat (inset of Figure 3a). Figure 3a shows the temperature-dependent I_G/I_{UV} of ZnO on the mat (at the center), which has subsequently been used for the evaluation of the temperature profile and mapping over the entire mat.

To probe the temperature, the PL spectra are recorded at the center of the CNT mat by applying a different bias to it. The variation of I_G/I_{UV} is shown in Figure 3b. By using the results of Figure 3a, we evaluate the variation of temperature with applied voltage as shown in the inset of Figure 3b (see the Supporting Informationfor a detailed description), which can be expressed by $T = 300 + aV^2$, as is the case of CNT bundles.[33] Figure 3c shows the optical images of luminescence of the ZnO coated CNT mat at different biases/temperatures. The decrease in the green band intensity is due to the increase in temperature. Overall, the quenched ZnO microcrystals can be used to find out the temperature at micrometer scale. It is believed that ZnO nanoparticles with similar properties can also be used for temperature sensing.

We also derive the temperature profile and perform the mapping of CNT mat at a constant bias of 2.6 V (Figure 3d,e). The variations of I_G/I_{UV} is deduced from the PL spectra taken at different places and evaluate the temperature profile of CNT mat using the results of Figure 3a (See the Supporting Information for a detailed description). It is observed that the temperature is maximum at the middle of CNT mat and decreases gradually towards the electrodes/edges. For example, the temperature is found to be about 502 K at the middle, about 429 K at electrode contacts, and about 491 K at the corners. The asymmetric variation of temperature is believed to be due to the non-uniform distribution of defects.[34] The larger the defect concentrations, the higher the resistance and thus the temperature. Furthermore, the non-uniform charge density as well as the electrical field leads to off-center heat dissipation,[34] and can cause the asymmetric variation of the temperature. We have also studied the melting temperature of indium (Supporting Information, Figure S7) to as an example of the practical application of ZnO temperature sensor of this type. The study on the temperature evolution in exothermic chemical reaction of H_2O and KOH (Supporting Information, Figure S8) suggests that the type of chemical reactions (exothermic or endothermic) and the reaction temperature can be obtained using non-contact optical probe thermometry.

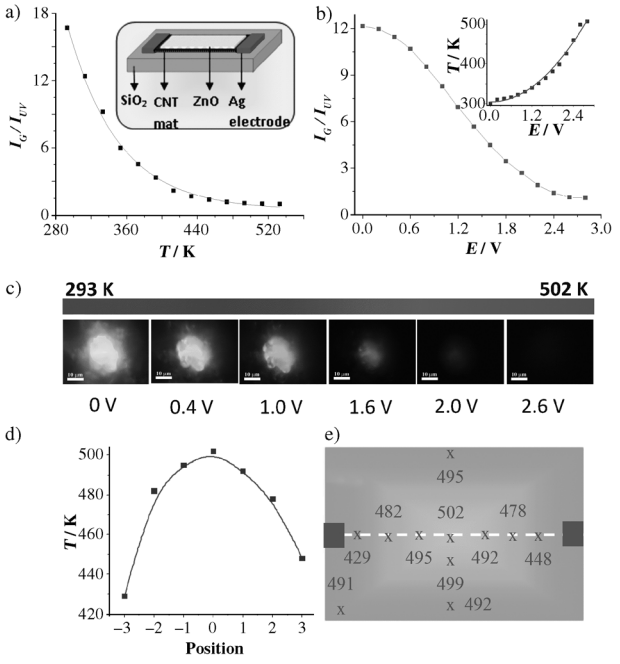

Figure 3. a),b) PL peak intensity ratio variation of ZnO/CNT mat structure (almost at the center) with temperature and voltage, respectively. The inset in (b) shows the variation of temperature with applied bias: experimental data with fitted line $T = 300 + 27.3\,V^2$. c) Optical images of luminescence of ZnO at different temperatures (293–502 K, realized by the application of different bias). Scale bars: 10 μm. d) Temperature profile along the dashed line shown in (e) for a bias of 2.6 V. Position "0" represents the middle of the mat. e) Representation of the temperature distribution over a CNT mat (3×2 mm^2).

In conclusion, green and intensely luminescent ZnO microcrystals have been synthesized from Zn powder by a thermal oxidation strategy. The PL spectra show a strong variation of intensity with temperature, which has been explored for temperature sensing in a temperature range of 83–473 K with a resolution of 0.1 K. This indicates that ZnO can be used in different temperature ranges such as cryogenic (< 298 K), physiological (298–318 K), and beyond with very high sensitivity. PMMA-ZnO is highly stable in comparison to bare ZnO. Non-contact thermometry is of high demand as is can also be used in electron microscopy, aerodynamic temperature sensing, temperature mapping, temperature-induced phase transition studies, type of chemical reactions, and many other applications. Overall, our results demonstrate the proof-of-concept for the green-luminescent ZnO irrespective of the size of the crystallites that can be used in cryogenic thermometry.

Experimental Section

Zn powder (Sigma Aldrich, 99.999% purity) was placed in a quartz boat and heated in horizontal-tube furnace in air. Yellow colored ZnO powders are obtained by vaporizing Zn powder at 1350°C for 30 min. and subsequent quenching. The morphology and phase of both ZnO samples are studied by scanning electron microscopy (SEM, Quanta 200), Raman spectroscopy with a 532 nm wavelength Nd:YAG laser (WITec 300) and X-ray diffraction (XRD, Panalytical X'Pert Pro diffractometer). The photoluminescence (PL) spectra at low/high temperature were recorded by WITec 300 with a 355 nm Nd:YAG laser. To obtain photoluminescence of individual microcrystals, a small amount of microcrystals are dispersed in isopropyl alcohol and drop-cast on a glass substrate. The optical photographs were taken using the WITec system after filtering the 355 nm light by a low-pass filter. The filter cuts off more than 95% of the incident light and passes only 5%. The PL imaging of individual microcrystal is performed by using confocal microscope (WITec system) equipped with an objective lens of Nikon S plan Fluor, ELWD 40X/0.60 NA.

Received: March 24, 2013
Revised: May 5, 2013
Published online: September 12, 2013

Keywords: cryogenic thermometry · luminescence · poly(methyl methacrylate) · sensors · ZnO microcrystals

[1] Y. H. Gao, Y. Bando, *Nature* **2002**, *415*, 599.
[2] W. Ryba-Romanowski, *J. Phys. Chem. Solids* **1993**, *54*, 153.
[3] J. Christoffersona, A. Shakouri, *Rev. Sci. Instrum.* **2005**, *76*, 024903.
[4] H. S. Peng, M. I. J. Stich, J. B. Yu, L. N. Sun, L. H. Fischer, O. S. Wolfbeis, *Adv. Mater.* **2010**, *22*, 716.
[5] F. Ye, C. Wu, Y. Jin, Y.-H. Chan, X. Zhang, D. T. Chiu, *J. Am. Chem. Soc.* **2011**, *133*, 8146.
[6] S. K. Singh, K. Kumar, S. B. Rai, *Sens. Actuators A* **2009**, *149*, 16.
[7] M. G. Cerruti, M. Sauthier, D. Leonard, D. Liu, G. Duscher, D. L. Feldheim, S. Franzen, *Anal. Chem.* **2006**, *78*, 3282.
[8] Y. Lan, H. Wang, X. Chen, D. Wang, G. Chen, Z. Ren, *Adv. Mater.* **2009**, *21*, 4839.
[9] D. Wawrzynczyk, A. Bednarkiewicz, M. Nyk, W. Strek, M. Samo, *Nanoscale* **2012**, *4*, 6959.
[10] C. D. S. Brites, P. P. Lima, N. J. O. Silva, A. Millan, V. S. Amaral, F. Palacio, L. D. Carlos, *Nanoscale* **2012**, *4*, 4799.
[11] R. J. Pylkki, P. J. Moyer, P. E. West, *Jpn. J. Appl. Phys.* **1994**, *33*, 3785.
[12] E. Saïdi, B. Samson, L. Aigouy, S. Volz, Peter Low, C. Bergaud, M. Mortier, *Nanotechnology* **2009**, *20*, 115703.
[13] C. D. S. Brites, P. P. Lima, N. J. O. Silva, A. Millán, V. S. Amaral, F. Palacio, L. D. Carlos, *Adv. Mater.* **2010**, *22*, 4499.
[14] J. Gallery, M. Gouterman, J. Callis, G. Khalil, B. McLachlan, J. Bell, *Rev. Sci. Instrum.* **1994**, *65*, 712.
[15] S. W. Allison, G. T. Gillies, *Rev. Sci. Instrum.* **1997**, *68*, 2615.
[16] S. Uchiyama, Y. Matsumura, A. P. de Silva, K. Iwai, *Anal. Chem.* **2003**, *75*, 5926.
[17] S. Chattopadhyay, P. Sen, J. T. Andrews, P. K. Sen, *J. Appl. Phys.* **2012**, *111*, 034310.
[18] B. Han, W. L. Hanson, K. Bensalah, A. Tuncel, J. M. Stern, J. A. Cadeddu, *Ann. Biomed. Eng.* **2009**, *37*, 1230.
[19] G. W. Walker, V. C. Sundar, C. M. Rudzinski, A. W. Wun, M. G. Bawendi, D. G. Nocera, *Appl. Phys. Lett.* **2003**, *83*, 3555.
[20] K. Okabe, N. Inada, C. Gota, Y. Harada, T. Funatsu, S. Uchiyama, *Nat. Commun.* **2012**, *3*, 705.
[21] S. Chenghua, X. Juan, W. Helin, X. Tianning, Y. Bo, L. Yuling, *Rev. Sci. Instrum.* **2011**, *82*, 084901.
[22] U. Ozgur, Y. I. Alivov, C. Liu, A. Teke, M. A. Reshchikov, S. Dogan, V. Avrutin, S.-J. Cho, H. Morkoç, *J. Appl. Phys.* **2005**, *98*, 041301.
[23] Y. W. Heo, D. P. Norton, S. J. Pearton, *J. Appl. Phys.* **2005**, *98*, 073502.
[24] H. Zeng, G. Duan, Y. Li, S. Yang, X. Xu, W. Cai, *Adv. Funct. Mater.* **2010**, *20*, 561.
[25] A. Shetty, K. K. Nanda, *Mater. Express* **2012**, *2*, 251.
[26] B. Cao, W. Cai, H. Zeng, *Appl. Phys. Lett.* **2006**, *88*, 161101.
[27] Y. P. Varshni, *Physica* **1967**, *34*, 149.
[28] L. Wang, N. C. Giles, *J. Appl. Phys.* **2003**, *94*, 973.
[29] J. Grabowska, A. Meaney, K. K. Nanda, J.-P. Mosnier, M. O. Henry, J.-R. Duclère, E. McGlynn, *Phys. Rev. B* **2005**, *71*, 115439.
[30] T. Voss, C. Bekeny, L. Wischmeier, H. Gafsi, S. Börner, W. Schade, A. C. Mofor, A. Bakin, A. Waag, *Appl. Phys. Lett.* **2006**, *89*, 182107.
[31] K. W. Liu, R. Chen, G. Z. Xing, T. Wu, H. D. Sun, *Appl. Phys. Lett.* **2010**, *96*, 023111.
[32] G. Baffou, P. Bon, J. Savatier, J. Polleux, M. Zhu, M. Merlin, H. Rigneault, S. Monneret, *ACS Nano* **2012**, *12*, 2107.
[33] L. T. Singh, K. K. Nanda, *AIP Adv.* **2012**, *2*, 022103.
[34] A. Liao, R. Alizadegan, Z.-Y. Ong, S. Dutta, F. Xiong, K. J. Hsia, E. Pop, *Phys. Rev. B* **2010**, *82*, 205406.

